Melt Spinning of Conducting Polymeric Composites Containing Carbonaceous Fillers

Martin Stråat,[1,2] Staffan Toll,[1] Antal Boldizar,[2] Mikael Rigdahl,[2] Bengt Hagström[1]

[1]*Swerea, Department of Textiles and Plastics, Box 104, Mölndal SE-431 22, Sweden*
[2]*Chalmers University of Technology, Department Of Materials and Manufacturing Technology, Göteborg SE-412 96, Sweden*

Received 1 April 2010; accepted 31 May 2010
DOI 10.1002/app.32882
Published online 27 September 2010 in Wiley Online Library (wileyonlinelibrary.com).

ABSTRACT: Fibers produced by melt spinning of conductive polymer composites are attractive for several applications; the main drawback is however reduced processability at high filler concentrations. Carbon nanotubes (CNTs) are considered suitable fillers for conductive polymer composites, replacing conductive grades of carbon black (CB). In this study, the fiber-forming properties of conductive polymer composites based on a conductive grade of CB and two masterbatches with CNT in a polyethylene matrix were investigated. The CB was also used in a polypropylene matrix for comparison. The rheological properties of the filler-containing melts in shear and their extensional behavior were evaluated. A piston-driven device was used to extrude the molten materials through a capillary; different capillary geometries were tested. Fibers were produced at various draw ratios, and their conductivity was determined. To assess the ultimate extensibility, a modified Rheotens method was used. The results showed that a conductive CB grade can have a lower percolation threshold and higher conductivity than a material with CNT. Conductivity decreased with increasing melt draw ratio for both types of fillers. The spinnability of the materials decreased with increasing concentration of filler material and correlations were found between spinnability and melt elasticity. © 2010 Wiley Periodicals, Inc. J Appl Polym Sci 119: 3264–3272, 2011

Key words: carbon nanotube; carbon black; polyolefins; rheology; drawing

INTRODUCTION

Electrically conductive fibers have long been used to provide antistatic characteristics in technical textiles and garments. Such fibers can be produced by melt spinning of a compound with small amounts of a suitable conductive filler, such as carbon black (CB).[1] The current technology appears, however, to be limited to moderate conductivities, well below 1 S/cm. It is desirable to achieve significantly higher conductivities in these textile fibers, exceeding 1 S/cm, which would make them useful in a wide variety of new applications, particularly in the area of functional and smart textiles.[2]

Electrical conduction in a carbon-filled polymer is a percolation phenomenon, i.e., high conductivity relies on the filler particles to form a network of unbroken conductive paths through the insulating polymer phase. This only happens above a critical filler concentration, the percolation threshold, typically a couple of percent by weight, where the conductivity increases rapidly by many decades over a narrow concentration range. Unfortunately, the formation of a percolating network also entails a rapid development of solid-like rheological properties such as elasticity and yield stress (frequently referred to as rheological percolation), which appears to be detrimental for spinnability by causing draw instabilities.[3] Thus, there exists a conflict between the quest for high conductivity and the rheological restrictions on spinnability.[1] The question arises as to whether or not this conflict is inevitable, i.e., is it possible to significantly exceed the electrical percolation threshold while retaining spinnability?

A promising alternative to CB is carbon nanotubes (CNTs), which have become commercially available relatively recently. These have a very large aspect ratio and therefore a potentially very low percolation threshold. Percolation thresholds as low as 0.01 wt % have been reported and 0.1 wt % seems to be practically achievable in the bulk composite.[4] Li et al.,[5] Li et al.,[6] and Pötschke et al.[7,8] showed that conductive fibers can be produced by melt spinning of CNT-filled polymers such as polypropylene (PP), poly(ethylene terephtalate), and polycarbonate. Li

Correspondence to: B. Hagström (bengt.hagstrom@swerea.se).

Contract grant sponsors: SSF (Swedish Foundation for Strategic Research), Vinnova (The Swedish Governmental Agency for Innovation Systems), the Smart Textiles Initiative.

et al.[6] obtained a conductivity (measured on extruded strands) above 0.001 S/cm at a CNT-content of 4 wt %. Both Haeggenmueller et al.[9] and Pötschke et al.[7] observed a loss of conductivity (measured on actual fibers) with increasing draw ratio because of the strong extension alignment of the nanotubes causing a loss of interparticle contacts. In several recent articles, however, the melt spinning process itself has not received any greater attention. Capillary dimensions and extrusion rates are rarely mentioned but could have a large influence on the obtained results.

The conductivity and percolation threshold also depend strongly on the degree of dispersion or deagglomeration.[10] Special techniques have been developed to improve the dispersion of CNTs. An effective dispersion technique involves *in-situ* polymerization directly onto the surface of the nanotubes followed by melt blending.[11–13] However, although such techniques lower the percolation threshold, they do not necessarily increase the conductivity at higher concentrations, since the polymer surface coating insulates the nanotubes by hindering their mutual contact.[10] Finally, we note that, to our knowledge, there is no report in the literature of melt spun CNT-filled polymer fibers with conductivities any higher than those achievable with CB.

Our objective presently is to understand more about the limitations on achievable conductivity put by spinning rheology, and whether it helps to use high aspect ratio fillers. We study the spinnability and the conductivity of PP or polyethylene (PE) filled with CB and CNTs. Rheological properties are also characterized, in an attempt to understand the role of the filler network with respect to spinnability. The CB used is a highly structured specialty grade for conductivity applications and one of the CNT-materials, a PE/CNT masterbatch, was produced by the aforementioned *in-situ* polymerization technique.

EXPERIMENTAL

Materials

A high-structure, conductive grade of CB grade, Ketchenblack EC 600JD (AKZO Nobel, Holland) with the aggregate size 10–50 nm, density 1800 kg/m^3, apparent bulk density 100–120 kg/m^3, BET surface area 1250 m^2/g, pore volume 480–510 cm^3/100 g, and pH 8–10, according to the supplier, was used. The PP grade was HG245FB (Borealis, Belgium) with a density of 910 kg/m^3 and a melt flow index (230°C/2.16 kg) of 26 g/10 min. The high-density polyethylene (HDPE), Aspun 6835A from Dow Chemical Company, Belgium, had a density of 950 kg/m^3 and a melt flow index (210°C/2.16 kg) of 17 g/10 min. Two masterbatches, based on HDPE and multiwalled carbon nanotubes (MWNT) were used to incorporate the nanotubes into the polymeric matrices; MB3520-00 from Hyperion Catalysis, USA, using Fibril^{TM} Nanotubes (denoted H-MWNT), and Nanocyl 9035 from Nanocyl, Belgium (denoted N-MWNT). The MB3520-00 masterbatch contained 20 wt % MWNT and the other masterbatch 31 wt % nanotubes (confirmed by thermogravimetric analysis). In case of the MB3520-00, the nanotubes were dispersed using melt compounding whereas in case of the other masterbatch the dispersion was achieved through *in-situ* polymerization of ethylene.

Compounding

The CB was dried at 120°C for 3 h in vacuum before compounding. For preparation of blends with CB, the following method was used. The polymer was melted and homogenized in a kneader (Brabender Plasticorder PLE 651, Germany) at 200°C and 60 rpm for 2 min before addition of CB. CB was added successively in three turns and compounded at 100 rpm for 10 min. For the preparation of polymers containing the MWNT-masterbatches, the matrix polymer was again first melted and homogenized in the kneader at 200°C and 60 rpm for 2 min. The masterbatch was then added in one turn and compounded at 100 rpm for 10 min.

Rheological measurements

The rheological measurements were performed with a cone-and-plate rheometer (CS Melt, Bohlin, Sweden) in the oscillating mode using a sinusoidal shear strain amplitude in the range 0.1–1%. The cone diameter was either 25 or 15 mm, depending on the filler loading, and the cone angle was 5.4°. The test temperature was 210°C, and the sample chamber was purged with nitrogen during the measurements. All material properties were measured at shear strains within the linear viscoelastic region. The angular frequency range covered in the experiments was from 0.06 to 200/s.

Elongational properties

A capillary viscometer (Rheoscope 1000, CEAST, Italy) equipped with a winding mechanism and a guiding wheel [Setup A, Fig. 1(a)] was used to evaluate the extensibility of the materials. The viscometer was also used without the guiding wheel and with a different winding mechanism [Setup B, Fig. 1(b)] to produce specimens for measuring the conductivity in both drawn state (fibers) and undrawn state (strands), further described below. Four different capillaries were used with the following dimensions: $L/D = 10/1$ (mm/mm), inlet angle 180° (flat

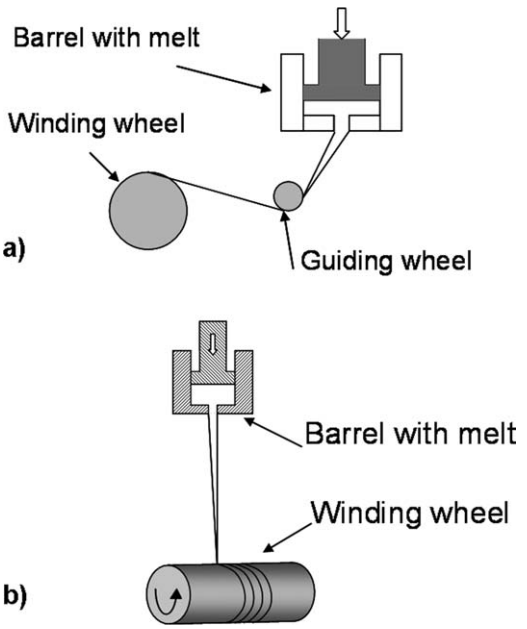

Figure 1 (a) Setup A for evaluating the maximum draw-down ratio for compounded materials with a low spinnability. (b) Setup B for melt spinning of fibers.

surface), $L/D = 10/1$, inlet angle 120°, $L/D = 5/1$, inlet angle 120°, and $L/D = 0.4/0.5$, inlet angle 30°, where L is the length and D is the diameter of the capillary. The extrusion rates (given as capillary exit velocities) were 0.2, 0.5, and 1 m/min with the capillaries with 1 mm diameter and 0.8, 2, and 4 m/min with the capillary with 0.5 mm diameter. The temperature was 210°C for all materials, although one material was also tested at 230°C. The velocity of the rotating disc was adjusted manually in small increments until the fiber ruptured. The draw ratio was taken as the ratio between the tangential velocity of the roll and the velocity of the extruded strand exiting the capillary. Draw-down ratios between 3 and 440 were obtained using this method. The ratio between the maximum circumferential velocity of the wheel (at rupture) and the exit velocity from the capillary was used as a measure of the maximum draw-down ratio or maximum melt draw ratio (MDR).

Samples for conductivity measurements

Setup A was not suitable for production of fibers using a high draw-down ratio. Samples for evaluating conductivity were therefore produced by winding the extruded strand on a rotating aluminum roll with a diameter of 100 mm placed 50 cm below the capillary exit [Setup B, Fig. 1(b)]. The circumferential speed of the take-up roll could be varied in the range 50–220 m/min giving draw-down ratios between 65 and 482 corresponding to fiber diameters in the range 40–110 μm. The capillary used for fiber production had $L/D = 10/1$ (mm/mm) with 180° inlet angle. The temperature used was 210°C and the piston speed 5 mm/min. The rotating disc device was however used to produce samples with low draw-down ratios (below 65). Undrawn samples (strands), approximately 10 cm in length, were produced by extruding and cutting specimens about 20 cm from the capillary.

Conductivity measurements

The electrical conductivity of the samples was measured with a two-point method. The undrawn strands were measured one by one. In case of the drawn fibers, a bundle of fibers (about 20 mg/cm) were contacted at both ends with silver paint. To ensure that all filaments were contacted, enough paint was applied to wet through the yarn completely. A voltage (U), was applied and varied between 5 (low resistance) and 450 V (high resistance), depending on the conductivity of the specimen, and the current (I) was measured using a Keithley solid-state electrometer model 602. The volume conductivity (σ_v) was calculated from the mass (m) of the fiber bundle (yarn) between the silver paint spots, the length (l) of the bundle and the measured voltage and current as

$$\sigma_v = \frac{\rho l^2 I}{U m} \tag{1}$$

where ρ is the calculated density of the filaments (922–994 kg/m^3 depending on the filler concentration).

RESULTS AND DISCUSSION

Rheological properties

Figure 2 shows the absolute value of the complex viscosity, the storage modulus, and the phase angle as a function of the frequency for the CB/PP composites (containing up to 16 wt % CB) at 210°C.

The effect of addition of CB on the rheological response of the material was substantial. Already at 2 wt % CB, the melts exhibited a clear viscosity enhancement at low frequencies. At higher CB-contents, the slope of the log(viscosity) − log(frequency) curves approached −1 in the lower frequency range, indicative of elasticity/yield stress.

The storage modulus clearly approached a constant value (plateau modulus) at low frequencies. This plateau was very pronounced at the higher concentrations, see Figure 2. The elastic character is also evident in the quite strong decrease in phase angle with increasing CB-content. At CB-loadings of 8 wt % and higher, the phase angle approached a

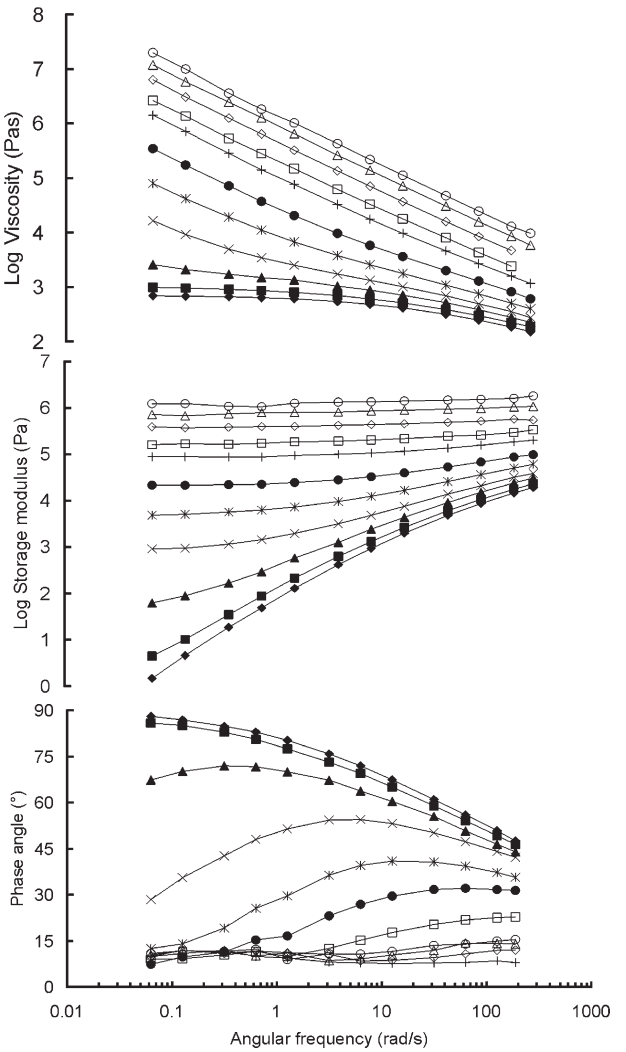

Figure 2 The absolute value of the complex viscosity (top), the storage modulus (middle), and the phase angle (bottom) versus the angular frequency for PP containing 0 (◆), 1 (■), 2 (▲), 3 (×), 4 (*), 6 (●), 8 (+), 10 (□), 12 (◇), 14 (△), and 16 (○) wt % CB. The temperature was 210°C.

constant value of around 10° over the entire frequency range studied. Similar results were obtained for CB/PE, N-MWNT/PE, and H-MWNT/PE materials, although the viscosity and elasticity enhancements began at different filler loadings.

The plateau storage modulus (G') is shown as a function of the filler content in Figure 3 for the different composites. In this region, G' could be related to the weight fraction of filler (w) with a power law type of relation, i.e.

$$G' \propto (w)^{\gamma} \tag{2}$$

The dependence of the plateau modulus on the weight fraction was very similar for CB/PP, CB/PE, and H-MWNT/PE and a common power law could be used for these composites with $\gamma = 4$. The plateau moduli of the PE-based composites containing N-MWNT were, however, about one order of magnitude larger than those of the other materials at any given filler loading and the power law exponent was lower ($\gamma = 3$).

To explain the elastic plateau, two possibilities are considered: (1) elasticity of the polymer, physically cross-linked by the filler, or (2) the elasticity of the particle network itself. In the first case, the elasticity is entropic and should thus be positively temperature dependent. The temperature dependencies of the complex viscosity (absolute value) and the storage modulus of CB/PP (4 wt %) and N-MWNT/PE (2 wt %) are shown in Figure 4. The other composites exhibited a similar behavior. Within the temperature range studied, an obvious temperature dependence of these viscoelastic parameters could only be discerned at frequencies higher than 1 rad/s, in which case it was a negative temperature dependence. This is strong evidence to rule out the first hypothesis (physical crosslinking), for CB as well as for MWNT. In support of the second alternative (intrinsic network elasticity), we may compare our results for the plateau modulus of the MWNT materials with the response of a pure CNT network (without matrix). Allaoui et al.[14] studied samples of vapor grown MWNTs in uniaxial compression, and found that the response can be described by Van Wyk's model[15] for compression of a mass of curly fibers:

$$P = k \cdot \phi^3 \tag{3}$$

where P is the applied pressure, φ is the CNT volume fraction, and k a curve fitting parameter. Given that $G' = c\varphi^n$, (where c and n are constants) and that n is of the order of 3–4, we find that $P(\varphi)$ and $G'(\varphi)$ are roughly equivalent functions:

$$P(\phi) \sim \int_0^{\phi} 3G'(\phi)\frac{d\phi}{\phi} = \frac{3G'}{n} \sim G'(\varphi). \tag{4}$$

It should be pointed out that at the low concentrations of fillers studied here, the use of weight fraction instead of volume fraction in eq. (2) will not have any significant influence of the value of the exponent n. Applying this relation to (eq. 3) yields shear moduli very similar to ours. We are thus led to the conclusion that it is the elasticity of the fiber network that is responsible for the low frequency plateau in the storage modulus, and that physical crosslinking plays a minor role.

Micromechanical models of fiber networks typically predict a power law of this type, with the exponent depending on the type of network structure. The case where fibers are straight on the length scale of the contact spacing along a fiber leads to

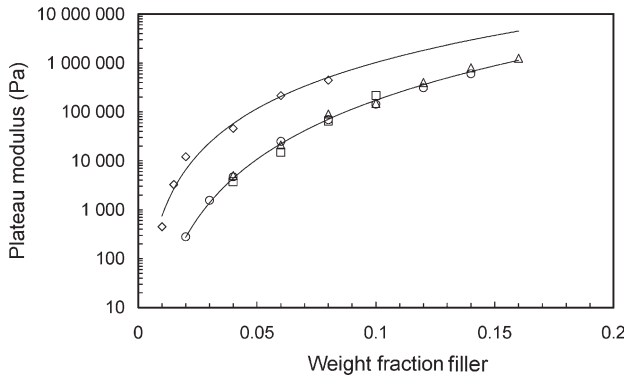

Figure 3 The plateau storage modulus versus weight fraction for CB/PP (△), N-MWNT/PE (◇), H-MWNT/PE (□), and CB/PE (○). The solid lines are least square fits of eq. (2).

$n \approx 5$[16] as compared to $n = 3$ for curly fibers. It is not surprising therefore, to find that these materials, whose radius of curvature is of the same order as the contact spacing ($\sim$ 100 nm) exhibit exponents in this range. Assuming the presence of Coulomb friction between the nanotubes (with friction coefficient $\sim$ 1), we also expect a yield stress $\tau_y(\varphi)$

$$\tau_y(\varphi) \sim P(\varphi) \sim G'(\varphi) \tag{5}$$

It will thus be assumed in the sequel that a plateau modulus implies a yield stress of similar magnitude.

The rheological behavior of the MWNT suspensions is thus fairly well understood. What is more puzzling is that the CB-material behaved very similarly, despite its completely different structure.

Spinnability

Spinnability is usually defined by how much the melt can be stretched without rupturing[17] i.e., the maximum MDR. Figure 5 shows the maximum MDR versus the filler concentration for CB/PE and N-MWNT/PE, obtained using Setup A with a capillary of length 10 mm, diameter 1 mm, inlet angle 180°, and extrusion rate 0.5 m/min. The (fuzzy) limit for practicable fiber production is also indicated in the Figure 5. These results show that fibers can be spun up to filler concentrations around 7 wt % for CB but only up to 2 wt % for N-MWNT with the set-up used. It can be noted that the maximum MDR-values for the unfilled HDPE and PP materials were higher than 800, which was the limit with Setup B. White and Tanaka[3] have suggested that the maximum MDR in filled systems is linked to a draw instability caused by the existence of a yield stress and, as discussed earlier, the yield stress is closely related to the elastic modulus (at least for the CNT-materials). We have therefore plotted the elastic plateau storage modulus from Figure 3 in the same graph as the maximum MDR-values, Figure 5. With increasing filler content, the maximum MDR value decreased whereas the modulus increased. The correlation between the two is far from perfect, but it certainly exists, and it is fair to say that the elastic modulus might serve as a rough indicator of spinnability. This is however further discussed later. The results with CB/PP and H-MWNT/PE were similar to CB/PE.

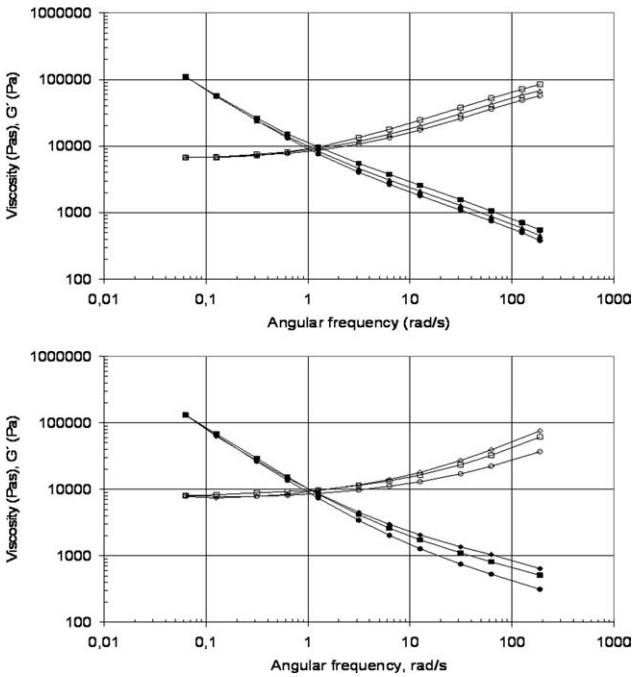

Figure 4 The absolute value of the complex viscosity (filled symbols) and the storage modulus (open symbols) as a function of the angular frequency for 4 wt % CB in PP (top) and 2 wt % N-MWNT in PE (bottom) at 170 (◇), 190 (□), 210 (△), and 230°C (○).

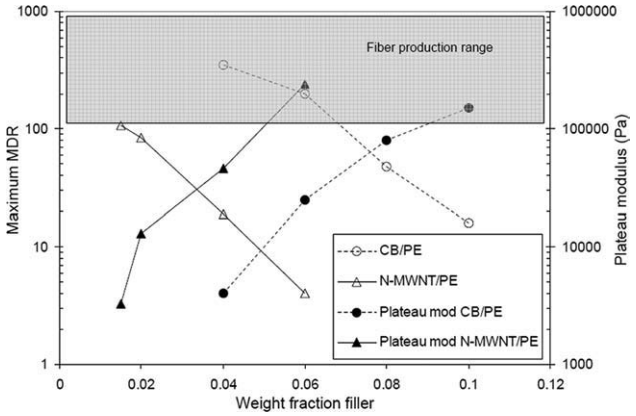

Figure 5 The maximum MDR obtained with Setup A and the plateau modulus for CB/PE and N-MWNT/PE measured at 210°C. Capillary dimensions were $L/D = 10/1$, inlet angle was 120°, and the extrusion rate was 0.5 m/min.

TABLE I
Influence of the Extrusion Rate and the Capillary Geometry on the Maximum MDR (Mean Value of Five Measurements), Measured at 210°C Using Setup A

Material	Extrusion rate (m/min)	Capillary geometry	Maximum MDR	Std. dev
4% CB/PE	0.2	$L/D = 5/1$, inlet angle 120°	335	88
4% CB/PE	0.5	$L/D = 5/1$, inlet angle 120°	261	60
4% CB/PE	0.5	$L/D = 10/1$, inlet angle 120°	352	58
4% CB/PP	0.2	$L/D = 10/1$, inlet angle 180°	396	52
4% CB/PP	0.5	$L/D = 10/1$, inlet angle 180°	200	11
4% CB/PP	0.5	$L/D = 10/1$, inlet angle 120°	193	8
4% CB/PP[a]	0.5	$L/D = 10/1$, inlet angle 120°	180	15
4% H-MWNT/PE	0.2	$L/D = 10/1$, inlet angle 120°	422	43
4% H-MWNT/PE	0.5	$L/D = 10/1$, inlet angle 120°	285	11
4% N-MWNT/PE	0.2	$L/D = 10/1$, inlet angle 120°	61	10
4% N-MWNT/PE	0.5	$L/D = 10/1$, inlet angle 120°	19	7
4% N-MWNT/PE	1	$L/D = 10/1$, inlet angle 120°	15	1.8
4% N-MWNT/PE	0.8	$L/D = 0.4/0.5$, inlet angle 30°	9	1.6
4% N-MWNT/PE	2.0	$L/D = 0.4/0.5$, inlet angle 30°	7	1.4
4% N-MWNT/PE	4.0	$L/D = 0.4/0.5$, inlet angle 30°	5	0.3

[a] Melt temperature 230°C, otherwise 210°C.

A draw instability phenomenon was also observed during the spinning experiments. A more or less pronounced periodic variation in fiber diameter was detected already at 2 wt % CB. The phenomenon resembles draw resonance but is more likely related to the yield stress: the stretching is confined to a sharp "necking" zone below the capillary exit, and the strand above this zone descends rigidly without being stretched. When the spin line force and gravity overcomes the yield stress, a second neck appears, leaving clumps of less stretched material like beads-on-a-string. A similar phenomenon was reported by White and Tanaka,[3] who also studied the influence of fillers such as CB on the maximum draw ratio and correlated it with melt spinning instabilities. All our materials did neck at some point along the spin line and quickly formed beads-on-a-string. For the N-MWNT, the spin line was very unstable and the instability occurred at lower filler loadings compared with the others.

As carefully pointed out earlier, the plateau modulus can only be used as a rough indicator of the spinnability. In addition, it is also to a great extent governed by the set-up used and the spinning conditions. Table I summarizes the spinnability results obtained with different extrusion rates and capillary geometries at a filler content of 4 wt %, using Setup A. Filler concentrations of 2 and 6 wt % were also used; yielding a similar behavior. In general, an increased extrusion rate (capillary exit velocity) reduced the attainable maximum MDR value.

The influence of the extrusion rate and the capillary geometry on the spinnability of some polyolefins associated with relaxation of polymer molecules within the capillary channel has been investigated by Laun and Schuch.[18] In the converging part of a die, elastic elongational strains will be imposed. If the melt subsequently flows through a parallel channel, relaxation will occur so that the orientations decay. The degree of relaxation will increase with increasing channel length and decreasing extrusion rate producing a less oriented melt exiting from the die, facilitating a higher MDR. The spinnability results of Laun and Schuch are in some cases in good agreement with the findings reported here, i.e., also when carbonaceous fillers were added. For example, higher maximum MDR values could be attained with a long capillary and a low extrusion rate. In the present case, there was a tendency towards lower maximum MDR values when using a longer tapered inlet of the capillary, but the results were actually within the experimental scatter (given by the standard deviation).

The number of experiments reported on in Table I is limited, but at similar processing conditions, the spinnability of CB/PE was clearly better than that of CB/PP, whereas H-MWNT/PE performed better in this respect than CB/PP, but somewhat poorer than CB/PE. The lowest degree of spinnability was obtained with N-MWNT which possibly can be associated with its higher plateau modulus. Increasing the temperature from 210 to 230°C in the case of CB/PP did not have any significant influence on spinnability. This may appear as somewhat surprising since it has been reported that an increase in temperature from 200 to 220°C had a large effect on the spinnability of a HDPE-grade.[19]

It is worthwhile to point to that the extrusion rate and the capillary geometry can have a significant effect on the spinnability even if the type and amount of filler is kept constant. This is exemplified by the N-MWNT/PE-system, Table I, for which the

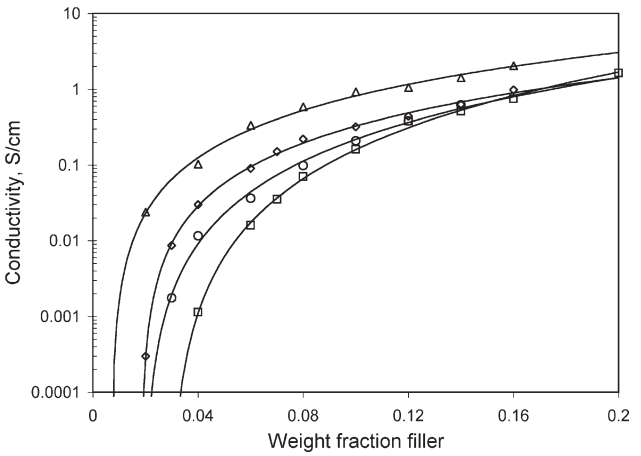

Figure 6 The electrical conductivity of the extruded strands versus the weight fraction of conductive filler; N-MWNT/PE (◇), CB/PP (△), CB/PE (○), H-MWNT/PE (□). The solid lines are least square fits of eq. (6) to the measured values.

maximum MDR value could be varied within an order of magnitude depending on the processing conditions and the experimental set-up.

Electrical properties

Figure 6 shows that the mean electrical conductivity of extruded strands (not drawn) of the different compounds increased with increasing filler content. Three samples were used for each value, the standard deviation was less than 10% of the mean value.

At a given filler content (below 10 wt %), the N-MWNT/PE-strands had the highest conductivity whereas the H-MWNT/PE exhibited the lowest and the CB-composites an intermediate level. At higher filler loadings, the conductivities of the different strands appeared to approach each other. In accordance with the classical percolation theory for a random system near the percolation threshold,[20] the conductivity values shown in the figure followed a power law:

$$\sigma = K(w - w_c)^{\beta} \tag{6}$$

where K is a constant related to the conductivity of the filler, w_c is the weight fraction at the percolation threshold, and β is the critical exponent. (Note again that the use of weight fractions instead of volume fractions has no significant bearing on the value of the exponent.) The constants in eq. (6) were determined by plotting the conductivity versus the reduced weight fraction, $(w - w_c)/w_c$, in a log–log diagram and fitting a straight line by means of least squares regression, maximizing the square of the correlation coefficient (R^2) by adjusting w_c. This enabled the evaluation of K, β, and w_c and the results are summarized in Table II.

It is well known that the electrical percolation threshold depends both on the particle shape (aspect ratio) and the degree of particle dispersion/deagglomeration.[10] It is also likely to depend on the interaction between filler and polymer during solidification (such as exclusion of filler particles from crystal lamellae). The percolation threshold values for CB/PP and CB/PE obtained here are on the low side for CB in polyolefins, although a threshold value of 2.5 wt % using the same CB-grade but a different PP was reported by King et al.[21] The threshold values of the H-MWNT/PE- and N-MWNT/PE-systems are slightly above the average values reported for these fillers.[10]

The critical exponents of polymers filled with CB and CNT reported in literature have been summarized by Kovacs et al.,[10] values between 2 and 3 seem to be the most frequent. According to the percolation theory, β is in the range 1.1–1.3 for two-dimensional systems and in the range 1.7–2 for three-dimensional random systems of mainly spherical particles.[22] The structure of both the CB/PP and the N-MWNT/PE composite (β = 1.8) can thus be interpreted in terms of a three-dimensional percolated carbon particle network. The H-MWNT/PE system clearly deviated by its significantly higher β-value (2.7). High critical exponents are often found for systems with high aspect ratio fillers, like carbon fibers and metal fibers.[22] The critical exponent for CB/PE was higher (2.3) than that of CB/PP (1.8). This difference was somewhat puzzling since the same CB-grade was used. The constant K in eq. (6) should, according to classical percolation theory, be related to the conductivity of the filler. The significant difference in K-values seen between CB/PP and CB/PE (account taken of different exponents) indicates a more complex nature of the conductivity development in the material. A different state of dispersion may have a large influence on the percolation.[10] It should however be noted, Figure 6, that the conductivity dependence on the filler concentration actually was quite similar for these two materials.

TABLE II
Parameters of eq. (6)

Material	CB/PP	CB/PE	N-MWNT/PE	H-MWNT/PE
Constant (K)	32	77	61	192
Percolation threshold (wt %) (w_c)	0.0182	0.0193	0.0070	0.0288
Critical exponent (β)	1.84	2.33	1.81	2.68

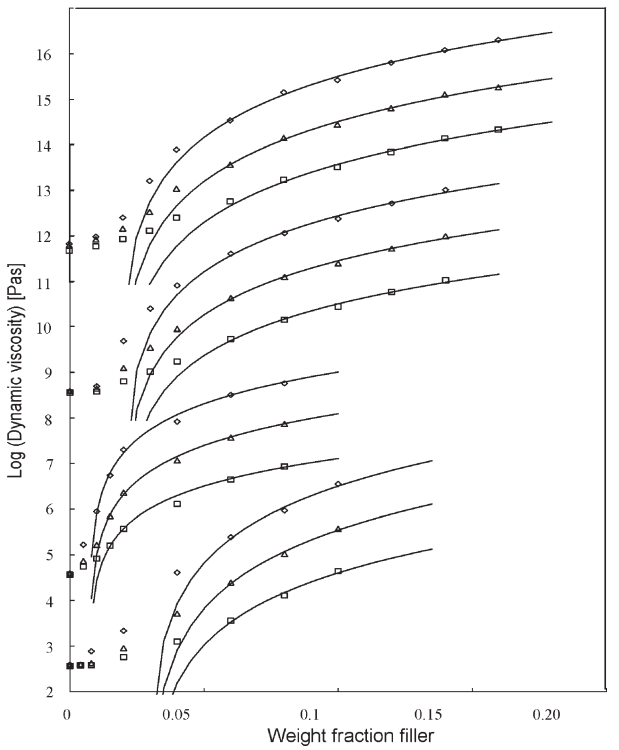

Figure 7 Magnitude of complex viscosity at 0.063 (◇), 0.63 (△), and 6.3 rad/s (□) at 210°C versus weight fraction of conductive filler. From top to bottom: CB/PP ($\times 10^9$), CB/PE ($\times 10^6$), N-MWNT/PE ($\times 10^2$), and H-MWNT/PE. The solid lines are power laws of the type $|\eta(\omega)| \sim (w - w_c)^{\alpha}$, where w_c is the electrical percolation threshold and α an adjustable constant. The three upper curves were shifted along the viscosity axis for clarity.

Finally, we show the magnitude of the complex viscosity at 0.063, 0.63, and 6.3 rad/s versus the weight fraction of conductive filler in Figure 7. Repeated viscosity measurements ($n = 3$) on the material with 4 wt % CB in PP indicated a variation of maximum 2% from the mean value.

The strong viscosity enhancement and the formation of an elastic network begin at different concentrations for the studied composites. It is possible to fit power laws of the type $|\eta(\omega)| \sim (w - w_c)^{\alpha}$ to the curves in Figure 7 at higher filler loadings by using the electrical percolation threshold (w_c) as critical concentration (here $\eta(\omega)$ denotes the complex viscosity). For CB/PP, CB/PE, and H-MWNT/PE, the exponent is about 3 whereas N-MWNT/PE exhibits an exponent close to 2 in accordance with the data in Figure 3. This correlation of electrical percolation with "rheological percolation" supports the notion of formation of a network of filler particles in intimate contact, mechanically and electrically.

The influence of the draw ratio on the conductivity

The electrical conductivity of melt-drawn monofilaments produced at different draw ratios is shown in Figure 8. The initial strands were produced with an exit velocity from the capillary of 0.5 m/min, the length and the diameter of the capillary was 10 mm and 1 mm, respectively, its inlet angle 180°, and the extrusion temperature 210°C. All of the materials lose conductivity with increasing draw ratio, presumably as a result of the destruction of the percolating network by separation and orientation of the conducting particles. The decrease was also more pronounced at low filler loadings, e.g., using a MDR of 100 in the case of 4 wt % CB/PE reduced the conductivity by three orders of magnitude, whereas in the case of 6 wt % CB/PE, the corresponding reduction was only one order of magnitude. Conductivities lower than about 10^{-5} S/cm could not be measured with the available equipment. Data points showing 10^{-5} S/cm could therefore be lower.

For the MWNT-materials, the conductivity decreased below detectable levels even at very low MDR. As shown by Pötschke et al.,[7] this is due to disruption of the network by extension-alignment of the nanotubes. The high sensitivity of MWNT on

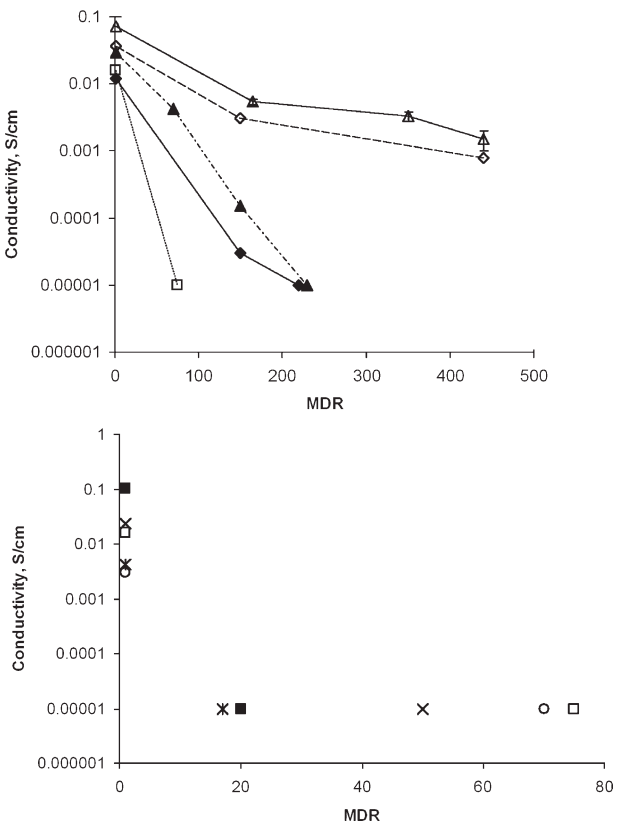

Figure 8 The conductivity versus the MDR for the drawn fibers. The following notations are used: 6 wt % CB/PE (◇), 6 wt % H-MWNT/PE (□), 6 wt % CB/PP (△), 4 wt % CB/PE (◆), 4 wt % CB/PP (▲), 4 wt % N-MWNT/PE (■), 2 wt % N-MWNT/PE (×), and 1.5 wt % N-MWNT/PE (○). The typical standard deviation is indicated for 6 wt % CB/PP, similar results were obtained for the other materials.

drawing is a serious disadvantage compared to CB when highly conductive fibers are sought for.

CONCLUSIONS

Suspensions of carbonaceous fillers in polymers exhibit solid-like equilibrium elasticity. We have shown that this is due to the elasticity within the immersed nanotube network, rather than physical crosslinking or immobilization of the polymer. In the case of nanotubes, the elastic moduli were shown to derive from bending elasticity in the nanotube network, with little influence from the polymer melt. However, the almost identical behavior of the CB network is hard to explain.

The spinnability (in terms of maximum MDR) is strongly affected by the filler concentration. Spinnability exhibits some correlation with the equilibrium elastic modulus, which points to plastic instability as a possible rupture mechanism. A draw instability phenomenon was observed, which caused diameter variations in the spun fibers. This too appears to be related to plasticity, in that it occurs in the same concentration range as the elastic plateau.

Electrical conductivity is well described by the power law of classical percolation theory, although the critical exponent was somewhat high for the H-MWNT/PE system. The critical exponent was also higher for CB/PE than for CB/PP, which seems difficult to reconcile with the percolation theory. Drawing has a negative influence on the electrical conductivity. For the CB materials the effect is likely due to particle chains being stretched apart. For the CNT materials the effect is massive, with a virtually complete loss of conductivity, probably due to the elongation alignment of the nanotubes.

In conclusion, any improvement of conductivity seems to somehow entail reduced spinnability, most likely because a high conductivity requires a dense network, which in turn implies higher elastic modulus and higher yield stress. Thus, the conductivity seems to remain well below 1 S/cm for anything that is spinnable. Using nanotubes as a filler does not seem to help. On the contrary, the nanotube materials after spinning had conductivity well below the CB materials.

References

1. Marcincin, A.; Hricová, M.; Fedorko, P.; Olejníková, K. Vlakna a textil 2005, 12, 98.
2. Wallace, G.; Campbell, T.; Innis, P. Fibers Polym 2007, 8, 135.
3. White, J. L.; Tanaka, H. J Appl Polym Sci 1981, 26, 579.
4. Bauhofer, W.; Kovacs, J. Compos Sci Technol 2009, 69, 1486.
5. Li, C.; Liang, T.; Lu, W.; Tang, C.; Hu, X.; Caoand, M.; Liang, J. Compos Sci Technol 2004, 64, 2089.
6. Li, Z.; Luo, G.; Wei, F.; Huang, Y. Compos Sci Technol 2006, 66, 1022.
7. Pötschke, P.; Brünig, H.; Janke, A.; Fischer, D.; Jehnichen, D. Polymer 2005, 46, 10355.
8. Pötschke, P.; Andres, T.; Villmow, T.; Pegel, S.; Brünig, H.; Kobashi, K.; Fischer, D.; Häussler, L. Compos Sci Technol 2010, 70, 343.
9. Haggenmueller, R.; Gommans, H.; Rinzler, A.; Fischer, J.; Winey, K. Chem Phys Lett 2000, 330, 219.
10. Kovacs, J.; Mandjarov, R.; Blisnjuk, T.; Prehn, K.; Sussiek, M.; Müller, J.; Schulte, K.; Bauhofer, W. Nanotechnology 2009, 20, 155703.
11. Claes, M.; Bonduel, D.; Pegel, S.; Alexandre, M.; Pötschke, P.; Dubois, P.; Luizi, F. NSTI Nanotech Technol Proc 2006, 1, 218.
12. Shaffer, M.; Koziol, K. Chem Commun 2002, 2074.
13. Cochet, M.; Maser, W.; Benito, A.; Callejas, M.; Martínez, M.; Benoit, J.; Schreiber, J.; Chauvet, O. Chem Commun 2001, 1450.
14. Allaoui, A.; Toll, S.; Evesque, P.; Bai, J. Phys Lett A 2009, 373, 3169.
15. Van Wyk, C. J Text Instit 1946, 37.
16. Alkhagenand, M.; Toll, S. J Appl Mech 2007, 74, 723.
17. Ziabicki, A. Fundamentals of Fibre Formation; Wiley: London, 1976.
18. Laun, H.; Schuch, H. J Rheol 1989, 33, 119.
19. Baldi, F.; Franceschini, A.; Riccó, T. Rheol Acta 2007, 46, 965.
20. Stauffer, D. Introduction to Percolation Theory; Taylor & Francis: London; 1985.
21. King, J.; Johnson, B.; Via, M.; Ciarkowski, C. J Appl Polym Sci 2009, 112, 425.
22. Weber, M.; Kamal, M. Polym Compos 1997, 18, 711.